Asymptotically universal crossover in perturbation theory with a field cutoff

2006 J. Phys. A: Math. Gen. 39 8681

(http://iopscience.iop.org/0305-4470/39/27/009)

INSTITUTE OF PHYSICS PUBLISHING JOURNAL OF PHYSICS A: MATHEMATICAL AND GENERAL

J. Phys. A: Math. Gen. **39** (2006) 8681–8697 doi:10.1088/0305-4470/39/27/009

Asymptotically universal crossover in perturbation theory with a field cutoff

L Li and Y Meurice[1]

Department of Physics and Astronomy, The University of Iowa, Iowa City, IA 52242, USA

E-mail: yannick-meurice@uiowa.edu

Received 20 July 2005, in final form 25 January 2006
Published 21 June 2006
Online at stacks.iop.org/JPhysA/39/8681

Abstract

We discuss the crossover between the small and large field cutoff (denoted as $x_{\max}$) limits of the perturbative coefficients for a simple integral and anharmonic oscillators. We show that in the limit where the order k of the perturbative coefficient $a_k(x_{\max})$ becomes large and for $x_{\max}$ in the crossover region, $a_k(x_{\max}) \propto \int_{-\infty}^{x_{\max}} \mathrm{e}^{-A(x-x_0(k))^2}\,\mathrm{d}x$. The order-independent constant A and the function $x_0(k)$ are determined empirically and compared with exact (for the integral) and approximate (for the anharmonic oscillator) calculations. Numerically, our best estimates are $A \simeq 1.5$, 1.3 and 1.2 for a λx^4, λx^6 and λx^8 perturbation respectively.

PACS numbers: 11.15.Bt, 12.38.Cy, 31.15.Md

1. Introduction

There has been a recent interest for quantum field theory models with a large field cutoff [1–4]. One motivation is that the convergence of perturbative series changes drastically [5, 6] if the large field configurations are removed from the path integral. This can be implemented, for instance, by removing configurations such that the norm of local fields exceeds some cutoff value. The field cutoff modifies the original problem; however, it has been found that for non-trivial ϕ^4 problems [6] the modified series apparently converge towards values which are exponentially close to the exact ones. In addition, at fixed order, it is possible in simple examples to choose the field cutoff in order to optimize the accuracy of the series at a given order [4, 7].

The calculation of the perturbative series for the modified theories where a large field cutoff is introduced is non-trivial. In the case of the anharmonic oscillator, approximate analytical methods [3] have been developed in the limits of large and small field cutoffs. Except at very low order, these methods are not accurate in the crossover region between these two

[1] Also at the Obermann Center for Advanced Study, University of Iowa, USA.

regimes, and it is necessary to develop new methods that are accurate. Fortunately, remarkable regularities were observed empirically: with appropriate rescalings and translations, the functions expressing the perturbative coefficients in terms of the field cutoff approximately collapse along a single curve [3].

As a side remark, we would like to point out that the collapse of properly rescaled curves sometimes indicates that a remarkable simplification occurs. A classic example is the equation of state relating the magnetization M and the magnetic field H in spin models. When M and H are rescaled by the appropriate power of $|T - T_c|$, the curves corresponding to various temperatures below (above) T_c collapse into a single curve characterizing the ordered (disordered) phase and universal relations among exponents or amplitudes follow. Note also that the collapse is only approximate and that non-universal corrections to scaling become important when $|T - T_c|$ is too large. Returning to the problem of interest here, a first and non-trivial step is to find an accurate description of the approximate collapse. This is the main point of this paper.

In section 2, we consider a simpler example, namely the perturbative series associated with a one variable integral, where a similar collapse is observed and can be modelled easily. In this case, we found a very good agreement between an empirical polynomial parametrization and a saddle point approximation. Generalizations of these results are discussed in section 3. Our main focus in this paper is to discuss the case of the quartic anharmonic oscillator ($V = (1/2)x^2 + \lambda x^4$) 'with a field cutoff' (the potential becomes infinite for $|x| > x_{\max}$). This model is introduced in section 4, and recent results regarding the behaviour of the perturbative coefficients [3] are briefly reviewed. Approximate Gaussian parametrizations of the crossover are introduced in section 5. Higher orders corrections are discussed in section 6 where a simple description emerges. The main result is that, for large order in perturbation, the transition from the small field cutoff to the large field cutoff regime can be expressed in terms of a 'universal' (order-independent) Gaussian integral.

The numerical determination of the coefficient of the quadratic term (the inverse square width of the Gaussian) is quite non-trivial, and an improved method to estimate this quantity is proposed in section 7. Perturbations of higher degree (λx^6 and λx^8) are treated with similar methods and compared in section 8. There remain small uncertainties in the determination of the quadratic coefficient of the Gaussian. Two possible conclusions (same coefficient for the three cases or coefficient decreasing with the degree of anharmonicity) are discussed. Finally, the possible relevance of the present observations for the interpolation between renormalization group fixed points is briefly discussed in section 9.

2. The simple integral

In this section, we discuss the calculation of the simple integral

$$Z(\lambda) = \int_{-\infty}^{\infty} \mathrm{d}x \, \mathrm{e}^{-\frac{1}{2}x^2 - \lambda x^4}. \tag{1}$$

In this example, introducing a field cutoff amounts to remove the integration tails where $|x| > x_{\max}$. Their contributions to the integral are less than $\sqrt{2\pi}\, \mathrm{e}^{-\lambda x_{\max}^4}$ and if $x_{\max}$ is large enough, we can approximate $Z(\lambda)$ with

$$Z(\lambda, x_{\max}) \equiv \int_{-x_{\max}}^{x_{\max}} \mathrm{d}x \, \mathrm{e}^{-\frac{1}{2}x^2 - \lambda x^4}. \tag{2}$$

If $x_{\max}$ is kept at a fixed finite value, the Taylor expansion of the exponential converges absolutely and uniformly over the domain of integration and it is legitimate to interchange

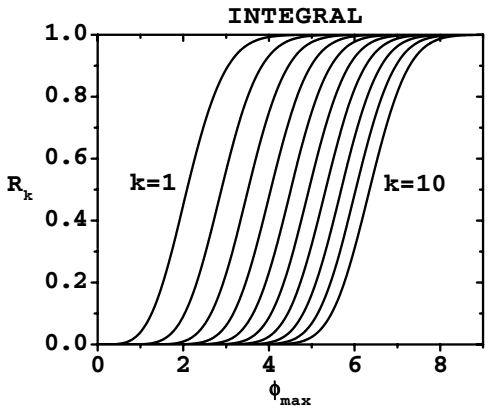

Figure 1. The ratio $R_k(x_{\max})$ as defined in equation (6). As k goes from 1 to 10, the curves move to the right.

the sum and the integral. The resulting series converges over the entire λ complex plane and reads

$$Z(\lambda, x_{\max}) = \sum_{k=0}^{\infty} a_k(x_{\max})\lambda^k, \tag{3}$$

with

$$a_k(x_{\max}) = \frac{(-1)^k}{k!} \int_{-x_{\max}}^{x_{\max}} \mathrm{d}x\, \mathrm{e}^{-\frac{1}{2}x^2} x^{4k}. \tag{4}$$

On the other hand, in the limit where $x_{\max} \to \infty$, we have

$$a_k(\infty) = \frac{(-1)^k}{k!} \Gamma\left(2k + \frac{1}{2}\right) (2)^{2k+\frac{1}{2}}, \tag{5}$$

and the coefficients grow factorially with the order which implies that the series diverges for any non-zero value of λ. In figure 1, we display the ratios

$$R_k(x_{\max}) \equiv \frac{a_k(x_{\max})}{a_k(\infty)} \tag{6}$$

for $k = 1$ to $k = 10$. As we can see, the curves corresponding to the different orders have a similar shape and move to the right as the order increases. Each curve can be characterized by three regimes: the low field cutoff regime, where the coefficient becomes very small, the large field cutoff regime where the coefficient reaches its asymptotic value and the crossover region. We now discuss each case separately.

2.1. The $x_{\max} \to \infty$ limit

When $x_{\max} \to \infty$, we can use integration by part recursively for the missing tails of integration in equation (4):

$$1 - R_k(x_{\max}) \simeq \mathrm{e}^{-\frac{1}{2}x_{\max}^2} \left[\frac{\left(\frac{1}{2}x_{\max}^2\right)^{2k-\frac{1}{2}}}{\Gamma\left(2k+\frac{1}{2}\right)} + \frac{\left(\frac{1}{2}x_{\max}^2\right)^{2k-\frac{3}{2}}}{\Gamma\left(2k-\frac{1}{2}\right)} + \cdots \right]. \tag{7}$$

At each integration by part, the argument of the Γ function at the denominator decreases by 1. Since the arguments are half integers, the process does not terminate. Using $1/\Gamma(x-1) = (x-1)/\Gamma(x)$, we end up with a factorial growth for the coefficients of the power series.

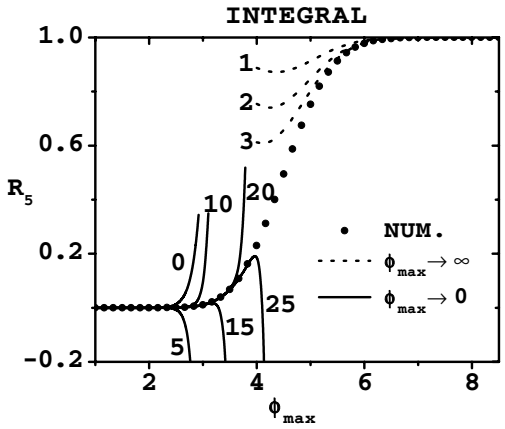

Figure 2. The ratio $R_k(x_{\max})$ in the large $x_{\max}$ and small $x_{\max}$ approximations. The dot stands for the accurate numerical result. The dash lines correspond to the large $x_{\max}$ approximation. The solid lines correspond to the small $x_{\max}$ approximation. The labels 1, 2, 3 correspond to the number of terms in equation (7). The six lines on the bottom left correspond to polynomial expansions when $x_{\max} \to 0$ from equation (8) with truncations at orders 0, 5, 10, 15, 20, 25.

2.2. *The $x_{\max} \to 0$ limit*

In the opposite limit where $x_{\max} \to 0$, we expand the exponential in equation (4) and we obtain the converging series in $x_{\max}^2$:

$$R_k(x_{\max}) = \frac{2\left(\frac{1}{2}x_{\max}^2\right)^{2k+\frac{1}{2}}}{\Gamma\left(2k+\frac{1}{2}\right)} \sum_{l=0}^{\infty} \frac{\left(-\frac{1}{2}x_{\max}^2\right)^l}{l!(4k+2l+1)}. \tag{8}$$

It is clear that the factorial growth of the denominator implies that this series converges over the entire $x_{\max}$ complex plane.

In figure 2, we show the curves corresponding to different orders in the two expansions discussed above, for $k = 5$. The small $x_{\max}$ region needs to be resolved logarithmically. If we restrict the expansion in equation (8) to $l \leqslant L$, for some given L, we note that the truncated series becomes a poor approximation when $x_{\max}$ reaches some critical value (almost independent of the order k in λ). This is illustrated in figure 3 for $L = 10$, where the critical value is near $x_{\max} \simeq 2.7$. One can roughly estimate this critical value by requiring that the Lth term is of the same order as the $(L-1)$th term. This yields the critical value $x_{\max} \simeq \sqrt{2L}$. A more accurate way to proceed is to determine the value of $x_{\max}$ for which the Lth order approximation becomes poor. The critical values of $x_{\max}$ can be fitted reasonably well with $0.63 + 0.64\sqrt{L}$. We can thus conclude that despite the fact that the series is convergent, many terms need to be calculated when the order becomes large. The number of terms that we need to calculate in order to get an accurate answer for a given $x_{\max}$ grows like $x_{\max}^2$.

2.3. *Approximate universality*

Figure 2 and the above discussion show that it is not easy to use the two expansions in the crossover region, which corresponds to the region where the integrand of equation (4) peaks. Using a saddle point approximation about the maximum of the integrand $x = \sqrt{4k}$, we obtain

$$R_k(x_{\max}) \simeq \frac{\int_0^{x_{\max}} \mathrm{d}x\, \mathrm{e}^{-2k+4k\ln(\sqrt{4k})}\, \mathrm{e}^{-(x-\sqrt{4k})^2+\cdots}}{\int_0^{\infty} \mathrm{d}x\, \mathrm{e}^{-2k+4k\ln(\sqrt{4k})}\, \mathrm{e}^{-(x-\sqrt{4k})^2+\cdots}}. \tag{9}$$

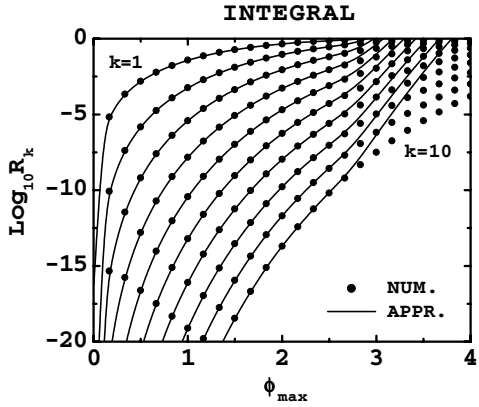

Figure 3. The numerical values (dots) of $\log_{10} R_k$ and the approximate values (lines) obtained with the small $x_{\max}$ expansion (8) with ten terms for $k = 1$ to $k = 10$.

If we only retain the quadratic term in the above expansion of the phase, we obtain what we call hereafter the Gaussian approximation. This approximation fails to reproduce the small $x_{\max}$ behaviour of equation (8). It is clear that far from the peak of the integrand, the Gaussian approximation is not good but it is in regions where the original integrand is very small. One can simplify this expression by adding the left tails of integration. This makes sense for k not too small, where it generates errors of the order $(4\sqrt{k})^{-1}\,\mathrm{e}^{-4k}$. For sufficiently large k, the following approximation holds for $x_{\max}$ not to far from $\sqrt{4k}$:

$$R_k(x_{\max}) \simeq \pi^{-1/2} \int_{-\infty}^{x_{\max}} \mathrm{d}x\, \mathrm{e}^{-(x-\sqrt{4k})^2}. \tag{10}$$

In equation (10), the only dependence on k is in the argument of the exponential. Its net effect is a translation in $x_{\max}$, and the shape of the function is universal (k-independent). In other words,

$$R_k(x_{\max}) \simeq U_{\mathrm{int}}(x_{\max} - \sqrt{4k}), \tag{11}$$

with

$$U_{\mathrm{int}}(x) \equiv \frac{\int_{-\infty}^{x} \mathrm{d}y\, \mathrm{e}^{-(y^2)}}{\sqrt{\pi}}. \tag{12}$$

If the assumption of universality expressed in equation (38) is approximately correct, the data should collapse into the universal curve when the argument of the kth-order curve is shifted by $\sqrt{4k}$. Figure 4 confirms that this is approximately the case. A more detailed look at figure 4 indicates that as the order increases, the shifted curve gets closer and closer to U_{int}. This limit is studied in the following section.

2.4. Order-dependent corrections

The basic approximation used to obtain U_{int} in the previous section is the saddle point approximation of the integral. We expanded the phase of the integrand

$$\Phi_k(x_{\max}) \equiv \ln R_k'(x_{\max}) \tag{13}$$

about its maximum up to second order. It is possible to improve this approximation by expanding to higher order:

$$-\frac{1}{2}x^2 + 4k \ln x = 2k(2\ln(2\sqrt{k}) - 1) - (x - \sqrt{4k})^2 - 4k \sum_{n=3}^{\infty} (1/n)[(\sqrt{4k} - x)/\sqrt{4k}]^n.$$

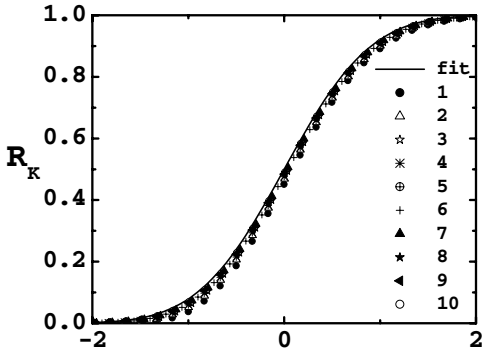

Figure 4. Same data as in figure 1 but with the argument of the kth-order curve shifted by $\sqrt{4k}$. The solid line is $U_{\rm int}$ of equation (12).

(14)

The series converges for $0 < x < 2\sqrt{4k}$. The even terms are negative and if we truncate at even orders, the integral of the exponential of the truncated sum converges when the bounds of integration are sent to infinity. As the order increases, the contribution of the two regions outside the radius of convergence are effectively cutoff, because the phase Φ_k becomes large and negative in these regions. For $x < 0$, this is desirable because there is no contribution from this region in the original integral. On the other hand, contributions from $x > 2\sqrt{4k}$ exist in the original integral. However, as we move from the maximum of the phase at $\sqrt{4k}$ to the edge of the radius of convergence at $2\sqrt{4k}$, the phase of the integrand drops by $(-6 + 4\ln 2)k \simeq -3.2k$ and the contribution of the right tail in the original integral is small, even for relatively small values of k.

In order to check the validity of this approach, we have calculated the phase Φ_k by using a discretized approximation of the derivative of R_k. We then fitted a set of points near the maximum with polynomials. The results were quite robust under changes in the number of points used, the degree of the polynomial and the spacing used to calculate the derivative. The second coefficient stabilized rapidly between -0.99 and -1 in agreement with equation (14). The coefficients of order 3 and 4 are shown in figure 5 where the good agreement with equation (14) is quite obvious.

The inclusion of the corrections of order 3 and 4 in the phase significantly reduces the small differences between $U_{\rm int}$ and the data in figure 4 and, for instance for $k = 5$, it is impossible to distinguish between the corrected integral and the data with the naked eye.

It is now clear how and why the agreement between the data and the simple guess $U_{\rm int}$ of equation (12) gets better as the order increases. The size of the crossover region is of order 1 and controlled by the quadratic term in the phase. In this region, for $|x - \sqrt{4k}| \sim 1$, $\Phi_k \simeq \text{const.} - (x - \sqrt{4k})^2$ because corrections of order $n > 2$ in equation (14) are suppressed by a factor $k^{1-n/2}$. On the other hand, the argument does not hold far away from the crossover, for $|x - \sqrt{4k}| \sim \sqrt{k}$, where a large number of terms are necessary to approximate logarithms in the phase that reproduce the correct power behaviour of the integral.

3. Remarks about the saddle point approximation

In this section, we generalize some aspects of the saddle point approximation used in the previous section. One important feature of the expansion of the phase given in equation (14) is that the coefficient of the quadratic term is k-independent and twice the value of the coefficient

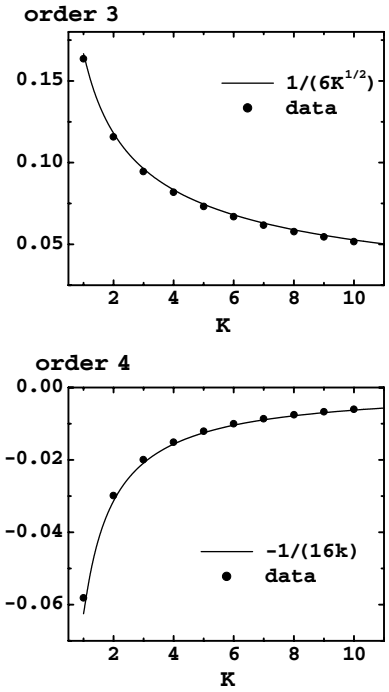

Figure 5. Values of the third and fourth coefficients of the Taylor expansion of the phase about its maximum obtained from polynomial fits compared with the predictions of equation (14).

of the quadratic term in the original integral. This has a very simple explanation. In general, $e^{-Ax^2}x^B$ is maximal at $x^* = \sqrt{B/2A}$, and we have the expansion

$$e^{-Ax^2}x^B \propto e^{-2A(x-x^*)^2+\cdots}. \tag{15}$$

In doing this calculation, one realizes that in the second derivative of the log estimated at x^*, the factors B cancel exactly. We want to emphasize that this 'non-renormalization' is due to the fact that the exponential is multiplied by a single power. If we consider instead $e^{-Ax^2}(x^B + \epsilon x^{B+\delta})$, then the exact cancellation does not hold. This can be checked at first order in ϵ, where x^* is changed according to

$$\sqrt{B/(2A)} \to \sqrt{B/(2A)}[1 + (\epsilon\delta/(2B))(B/(2A))^{\delta/2}], \tag{16}$$

and the coefficient of the quadratic term in the expansion of the phase is changed according to

$$-2A \to -2A[1 - (\epsilon\delta^2/(2B))(B/(2A))^{\delta/2}], \tag{17}$$

and becomes B-dependent (except if $\delta = 2$ or 0).

4. The anharmonic oscillator with a field cutoff

Our main objective in this paper is to understand the crossover for the anharmonic oscillator. The model has been studied in detail in [3]. Note that another modified anharmonic oscillator where λx^4 becomes $\lambda x^4_{\max}$ (instead of $+\infty$ here) for $|x| \geqslant x_{\max}$ is discussed in [8]. We introduce some notations and briefly review some basic results. For convenience, we use quantum mechanical notations instead of field theoretical ones. The 'field' will be denoted as x instead of ϕ and the field cutoff will be denoted as $x_{\max}$. In quantum mechanics language,

it means that the potential becomes infinite at $\pm x_{\max}$. We use units such that $\hbar, \omega$ and the 'mechanical mass' m are 1. If the dependence on these three quantities were restored, dimensionless quantities would be expressed in terms of $\sqrt{\omega m/\hbar}x_{\max}$ and $\hbar\lambda/m^2\omega^3$. The Hamiltonian reads

$$H = \frac{p^2}{2} + V(x) \tag{18}$$

with

$$V(x) = \begin{cases} \frac{1}{2}x^2 + \lambda x^4 & \text{if } |x| < x_{\max} \\ \infty & \text{if } |x| \geqslant x_{\max}. \end{cases} \tag{19}$$

We will consider the perturbative expansion of the ground state:

$$E_0(x_{\max}, \lambda) = \sum_{k=0}^{\infty} E_0^{(k)}(x_{\max})\lambda^k. \tag{20}$$

As in section 2, we use the notation R_k for the kth coefficient in units of its usual value:

$$R_k(x_{\max}) \equiv E_0^{(k)}(x_{\max}) \big/ E_0^{(k)}(\infty). \tag{21}$$

We have shown [3] that in the limit of small $x_{\max}$,

$$R_k(x_{\max}) \propto x_{\max}^{6k-2}, \tag{22}$$

while in the limit of large $x_{\max}$,

$$1 - R_k(x_{\max}) \propto x_{\max}^{4k+1}\, \mathrm{e}^{-x_{\max}^2}. \tag{23}$$

5. Gaussian approximations of the crossover

In this section, we discuss Gaussian approximations of the crossover in a way similar to what was done in section 2.3 for the integral. From equation (23), we expect that in the large $x_{\max}$ limit, we have at leading order

$$R_k'(x_{\max}) \propto x_{\max}^{4k+2}\, \mathrm{e}^{-x_{\max}^2}. \tag{24}$$

If we now extrapolate backwards this behaviour at intermediate values of $x_{\max}$ (this is of course an approximation), $R_k'(x_{\max})$ has a maximum at

$$x_*(k) \equiv \sqrt{2k+1}. \tag{25}$$

Expanding the logarithm up to order 2 about this point, we obtain the Gaussian approximation:

$$R_k'(x_{\max}) \propto \mathrm{e}^{-2(x_{\max} - x_*(k))^2}. \tag{26}$$

With this approximation, we have $R_k''(x_*(k)) = 0$. This approximate prediction for the value of x for which the second derivative vanishes can be compared with the accurate numerical value, denoted by $x_0(k)$, for which it actually vanishes. The numerical values can be found in table 2 of [3] and are shown in figure 6, together with approximate analytical formulae. Typically, $x_0(k) \simeq x_*(k)$ with a 10% accuracy for $k \leqslant 10$. A more accurate formula can be found by fitting $x_0(k)^2$ with a linear function. Using the data for $k = 2$ to 10, we obtain $x_0(k) \simeq \sqrt{1.63k + 3.26}$. Using the data for $k = 10$ to 20, we obtain a slightly different fit that we expect to be closer to the asymptotic behaviour:

$$x_0(k) \simeq \sqrt{1.61k + 3.48}. \tag{27}$$

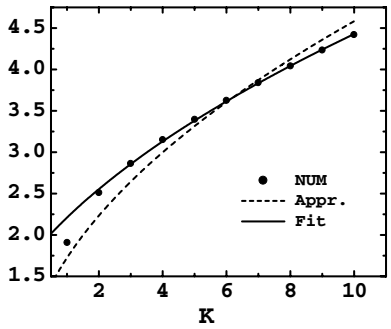

Figure 6. The numerical values of $x_0(k)$ (circles) compared to $\sqrt{2k+1}$ (dash line) and $\sqrt{1.63k+3.26}$ (solid line).

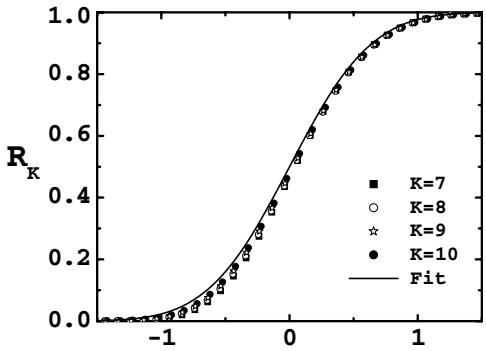

Figure 7. $R_k(x_+x_0(k))$ for $k = 7, \ldots, 10$ and the function $U_{\mathrm{anh},1}(x)$ of equation (29).

In [3], we found that if $R_k(x_{\max})$ is translated by $x_0(k)$, the data for $k = 2, \ldots, 10$ approximately collapse. In other words,

$$R_k(x + x_0(k)) \simeq U_{\mathrm{anh}}(x). \tag{28}$$

An approximate form for $U_{\mathrm{anh}}(x_{\max})$ is suggested by equation (26). Integrating and normalizing by requiring $\lim_{x\to+\infty} U_{\mathrm{anh}}(x) = 1$, we obtain

$$U_{\mathrm{anh},1}(x) \simeq \sqrt{2/\pi} \int_{-\infty}^{x} \mathrm{d}y\, \mathrm{e}^{-2y^2}. \tag{29}$$

We have used the subscript anh, 1 to indicate that it is a first approximation and that a better form will be found later. This proposal is compared with the empirical data for $k = 7, \ldots, 10$ in figure 7. We only displayed a few values of k so that it is possible to distinguish the various orders on the graph. One can see that the collapse of the various curves is reasonably good. The function $U_{\mathrm{anh},1}$ fits the collapsed data quite well on the upper right, but appears to be slightly above the data on the lower left. However, as the order increases (in figures 7 to 10), the difference diminishes.

The reason why $\sqrt{2k+1}$ is not a very good approximation of $x_0(k)$ is that the large $x_{\max}$ behaviour given by equation (24) is not accurate for intermediate values of $x_{\max}$. Studying numerically the behaviour of

$$R_k(x_{\max})\, \mathrm{e}^{x_{\max}^2}, \tag{30}$$

near $x_0(k)$, one obtains a very good linear behaviour on a log–log plot. If equation (24) were correct, the slope would be $4k + 2$. However, collecting the slopes for various values

of k, one concludes that $4k + 2$ should be replaced by $3.2k + 7.8$ in equation (24). This is consistent with the empirical form of $x_0(k)$ of equation (27) which is approximately the square root of one half of this fit (see section 3 with $A = 1$). When studying the difference between equation (30) and its approximation by a single power, one notices small quadratic corrections. We will not report all the details of this investigation, but only mention that these quadratic corrections can be approximately removed by replacing equation (30) by $R'_k(x_{\max})\, e^{\beta_k x_{\max}^2}$ and adjusting the value of β_k to the value for which the quadratic corrections change sign.

We conclude that a more realistic version of equation (24) is

$$R'_k(x_{\max}) \propto x_{\max}^{3.2k+7.8}\, e^{-\beta_k x_{\max}^2}. \tag{31}$$

The results of section 3 suggest that e^{-2y^2} should be replaced by $e^{-2\beta_k y^2}$ in equation (29). This brings an explicit dependence on k, and universality can only be reached asymptotically if β_k tends to a limit when k becomes large.

Empirically, the values of β_k are slightly larger than 1 for $k < 10$ and slightly smaller than 1 for $k > 10$. This modification allows us to reduce the small discrepancies of the Gaussian approximation used before. Note that in figure 7, the closeness of $k = 9$ and 10 to $U_{\text{anh},1}$ reflects the fact that β_9 and β_{10} are very close to 1. β_k is closely related to $A_k^{(2)}/2$, a quantity that will be studied in the following section. Anticipating the results presented there, we expect that as k increases, β_k stabilizes to a value close to 0.75.

The limitations of the Gaussian approximation, or of any other expression of a universal function U as the integral of a even function, can be seen from the duality relation which exchanges the small and large field cutoff regions

$$U(-x) = 1 - U(x), \tag{32}$$

which cannot be exact since the approach of 0 when $x_{\max} \to 0$ is power like while in the large $x_{\max}$ limit, the approach of 1 is exponentially small. In at least one of these two limits, U should fail to provide the correct behaviour.

6. Numerical study of the higher order corrections

The complexity of the exact form of the terms of the perturbative series increases rapidly with the order (see for instance [9] for an exact expression up to order 4). The number of graphs grows factorially [10]. It seems unlikely that at this point one could guess approximate equations such as equation (31), or an improved version of it, from analytical expressions at large order. For this reason, we will describe $\ln(R'_k)$ near $x_0(k)$ using polynomial approximations. This method is numerically robust and has been tested successfully in the case of the integral where the expansion can be calculated analytically. Our main working assumption is that in the vicinity of $x_0(k)$,

$$\ln(R'_k(x)) \simeq \sum_{q=0}^{Q} A_k^{(q)} (x - x_0(k))^q. \tag{33}$$

Note that the presence of odd powers in the expansion breaks the duality expressed in equation (32). The fitted value for the largest order ($q = Q$) coefficient is typically not very stable and as we want to focus on the terms with $q = 2$, 3 and 4, we have used $Q = 5$, 6 and 7. We then checked that the terms $A_k^{(q)}$, for $q = 2$, 3 and 4, were quite stable under small changes as in section 2. They are displayed in figure 8.

As $A_k^{(q)}$ seem to reach asymptotic values with power corrections, we have fitted the larger k values with the parametric form

$$A_k^{(q)} = a^{(q)} + b^{(q)} k^{-c^{(q)}}. \tag{34}$$

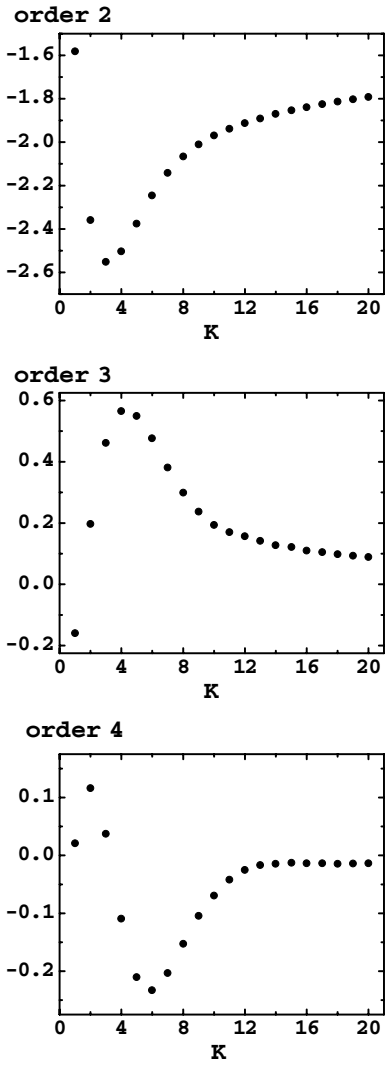

Figure 8. $A_k^{(q)}$ for $q = 2$, 3 and 4 and $k = 1, \ldots, 20$.

Other parametric forms, such as an exponential decay, have been tried too but shown to have a significantly larger chi-square. We first estimated $c^{(q)}$ by making a log–log plot of $\left|A_{k+1}^{(q)} - A_k^{(q)}\right|$, and then obtained $a^{(q)}$ and $b^{(q)}$ with standard linear fit methods. Slightly better fits can be obtained by using directly a nonlinear fit based on equation (34). We performed the fits with different sets of $A_k^{(q)}$ with k running from k_0 to 20. The results showed a regular dependence on k_0: as k_0 increased, the three fitted parameters showed small, monotonic changes and we then attempted an extrapolation assuming a dependence on k_0 of the form (34). This second extrapolation is much more delicate as we will see below.

The stability of the method was checked by using five different sets of $A_k^{(q)}$ obtained with slightly different procedures: changes in the range of $x_{\max}$ used in the fits of equation (33), changes in $\Delta x_{\max}$ used to calculate the derivative of R_k, changes in $Q = 5$ or 6. We found that the coefficients $A_k^{(q)}$ (the typical errors are a few parts in a thousand or less)

and the fit parameters $a^{(q)}$, etc (the typical errors are a few parts in a hundred) were quite stable; however, the numerical errors on the fit parameters do not always allow us to estimate properly the dependence on k_0 discussed above.

For $q = 2$, the fits at fixed k_0 were found to be quite consistent among the five sets and the second extrapolation in k_0 was in some cases possible. Our final estimate is

$$A_k^{(2)} \simeq -1.5(1) - 2.0(1)k^{-0.6(1)}, \tag{35}$$

with the parentheses indicating the estimated error on the last written digit. Given our lack of systematic understanding of the k_0 dependence, the errors may be larger. This question will be readdressed in the following section.

For sufficiently large k, we found that $A_k^{(2)} \simeq -2\beta_k$ as defined in the previous section. It is clear from figure 8 that for $k \simeq 10$, $A_k^{(2)} \simeq -2$ is in agreement with the observation $\beta_{10} \simeq 1$. To give an idea about the accuracy of the agreement, for $k = 15$, $A_{15}^{(2)} \simeq -1.866$ while $\beta_{15} = 0.938 = 1.876/2$.

For $q = 3$, more variations among the five data sets were observed. A tentative value for $a^{(3)}$ is 0.02(1). However, this is more than four time less than $A_{20}^{(3)} \simeq 0.089(1)$. More stable results with consistent extrapolations were obtained by setting $a^{(3)} = 0$. Our final estimate is

$$A_k^{(3)} \simeq 1.3(3)k^{-0.9(1)}. \tag{36}$$

We repeat that it is difficult to rule out a small positive value asymptotically. The decay rate seems faster than in the single power case studied in section 3 where $A_k^{(3)} \propto k^{-1/2}$. In our fits, the average value of the power was -0.94 for $k_0 = 17$ and the extrapolated value the farther away from this average was -0.86.

For $q = 4$, stronger variations among the five sets were observed. In all cases $a^{(4)}$ was much smaller than $A_{20}^{(4)} \simeq -0.017(1)$ and with no consistent sign. More stable results with reasonably consistent extrapolations were obtained by setting $a^{(4)} = 0$. Our final estimate is

$$A_k^{(4)} \simeq -1.5(6)k^{-1.3(3)}. \tag{37}$$

We have also considered the coefficients for larger values of q and found that they also appear to reach zero asymptotically. Their values are in general quite small. For instance, $A_{20}^{(5)} \simeq 0.004$ and $A_{20}^{(6)} \simeq -0.0007$.

We conclude that for k being sufficiently large and $x_{\max} = x_0(k) + x$, with x of order 1, we have in good approximation that

$$R_k(x_0(k) + x) \simeq U_{\text{anh}}(x) \simeq \sqrt{A/\pi} \int_{-\infty}^{x} \mathrm{d}y\, \mathrm{e}^{-Ay^2}, \tag{38}$$

with $A \simeq 1.5$. The words of caution regarding this 'limit' are the same as in the case of the integral: if $|x|$ is too large, the non-Gaussian corrections need to be taken into account. In the above discussion, our best guess for the error on A is 0.1; however, our understanding of the corrections to equation (34) is limited and the error may be larger.

7. Alternate estimation method

In order to eliminate the dependence on k_0 found in the previous section, we have considered 'quasilocal' estimators of the three unknown parameters appearing in equation (34):

$$c_k^{(q)} \equiv -1 - 2k \frac{A_{k+1}^{(q)} - 2A_k^{(q)} + A_{k-1}^{(q)}}{A_{k+1}^{(q)} - A_{k-1}^{(q)}} \tag{39}$$

Table 1. The estimators $a_k^{(2)}$, $b_k^{(2)}$ and $c_k^{(2)}$ for a λx^4 perturbation. Unless specified by parentheses, an error of 1 or less on the last printed digit is assumed.

k	$a_k^{(2)}$	$b_k^{(2)}$	$c_k^{(2)}$
10	−1.73	−11.0(2)	1.64(2)
11	−1.74	−11.0(8)	1.65(4)
12	−1.71	−7.8(9)	1.46(6)
13	−1.70	−6.2(2)	1.34(2)
14	−1.68	−4.9(4)	1.21(4)
15	−1.63	−3.3(2)	0.99(4)
16	−1.61	−3.0(2)	0.91(3)
17	−1.57	−2.3	0.76(2)
18	−1.55	−2.1	0.71(2)
19	−1.51	−1.9	0.63

$$b_k^{(q)} \equiv -k^{c_k^{(q)}+1}\left(\frac{A_{k+1}^{(q)} - A_{k-1}^{(q)}}{2c_k^{(q)}}\right) \tag{40}$$

$$a_k^{(q)} \equiv A_k^{(q)} - b_k^{(q)} k^{-c_k^{(q)}}. \tag{41}$$

If we *assume* that equation (34) is exact, *then*

$$c_k^{(q)} = c^{(q)} - \frac{((c^{(q)})^2 - 1)(c^{(q)} + 2)}{12k^2} + \mathcal{O}(k^{-4}). \tag{42}$$

For the range of values of c considered here ($c < 2$) and $k > 10$, the $\mathcal{O}(k^{-2})$ term is less than 0.01. Consequently, variations significantly above 0.01 in $c_k^{(q)}$ indicate the presence of corrections to the simple power decay of equation (34) or numerical fluctuations. The empirical values of the estimators for $q = 2$ are given in table 1. The estimated numerical errors on the last printed digit appear in parentheses (the default being (1)). These errors have been estimated by performing the calculations with slightly different intervals, changing Q or $\Delta x_{\max}$. Five sets of estimators were used to produce the tables. The variations of $c_k^{(q)}$ indicate that corrections to equation (34) are present. However, we were not able to find a stable extrapolation in k using an asymptotic behaviour of the form (34). Note that the last row of table 1 is quite consistent with our estimates of the previous section.

Similarly, we can find quasilocal estimators when $a^{(q)} = 0$ is assumed. We use a hatted symbol to distinguish them from the previous ones:

$$\widehat{c}_k^{(q)} \equiv -k\frac{A_{k+1}^{(q)} - A_{k-1}^{(q)}}{2A_k^{(q)}} \tag{43}$$

$$\widehat{b}_k^{(q)} \equiv k^{\widehat{c}_k^{(q)}} A_k^{(q)}. \tag{44}$$

The numerical results are shown in table 2 for $q = 3$. Again no stable extrapolation was found, but the last line is in good agreement with our previous estimates.

In summary, the method presented here is simpler, allows a good control of the numerical errors and is consistent with the previous one. A better understanding of the asymptotic behaviour of the estimators would require longer series, more accurate data or a better understanding of the nature of the corrections to equation (34). Note that with only a few exceptions, the estimators increase (or decrease) monotonically, and consequently it seems reasonable to treat the last row of the tables as a lower (or a upper) bound.

Table 2. The estimators $\widehat{b}_k^{(3)}$ and $\widehat{c}_k^{(3)}$ for a λx^4 perturbation. Unless specified by parentheses, an error of 1 or less on the last printed digit is assumed.

k	$\widehat{b}_k^{(3)}$	$\widehat{c}_k^{(3)}$
10	9.7(2)	1.68
11	7.0	1.54
12	5.0	1.39
13	3.8	1.29
14	2.8	1.17
15	2.3	1.09
16	2.0	1.04
17	1.74(2)	0.995(3)
18	1.61(3)	0.966(3)
19	1.49(2)	0.940(1)

8. Extension to λx^{2N} perturbations

We have repeated the calculations of sections 6 and 7 for a λx^6 and a λx^8 perturbation. We found patterns qualitatively very similar to those for a λx^4 perturbation. At a quantitative level, we found two differences. The first one is that, for a fixed order k, the values $x_0(k)$ of the crossover point, where the second derivative of R_k vanishes, are larger. For a λx^6 perturbation, we found $x_0(k) \simeq \sqrt{2.9 + 2.7k}$ and for a λx^8 perturbation, $x_0(k) \simeq \sqrt{2.7 + 3.7k}$. Second, the decay of corrections to the asymptotic Gaussian behaviour becomes slower as the degree of anharmonicity increases. Since our numerical method is based on power expansion [3], large values of $x_{\max}$ stretch the limit of a PC's virtual memory. For this reason, we have limited our investigation to values of $x_{\max}$ up to 8. For this maximal value of $x_{\max}$, we were able to fit reliably the crossover behaviour of coefficients up to order 15.

The results for $q = 2$ are shown in table 3. Our main interest is to determine the asymptotic value of $a_k^{(2)}$. The changes in this quantity are monotonic. For λx^6, $\left|a_k^{(2)}\right|$ keeps decreasing. If this feature persists, $\left|a_k^{(2)}\right| < 1.3$. For λx^8, $\left|a_k^{(2)}\right|$ keeps increasing. If this feature persists, $\left|a_k^{(2)}\right| > 1.22$. We cannot exclude the possibility that both estimators could stabilize at an intermediate value. If this value is potential independent, then the estimator for λx^4 is farther from its asymptotic value when $k = 19$ than the estimator for the higher degree perturbation when $k = 14$.

For $q = 3$, the data are consistent with $a^{(3)} = 0$ and we have used the hatted estimators of section 7. The results are shown in table 4. In both cases, the changes end up being close to the numerical errors which was not the case for the λx^4 case even at larger values of k.

In summary, we found that for a λx^6 and a λx^8 perturbation, the crossover can asymptotically be described by the integral of a Gaussian. The coefficient of the quadratic term, the large k limit of $a_k^{(q)}$, denoted by A in equation (38), could possibly be a number independent of the degree of anharmonicity. If this is the case, it is plausible that this value would be near 1.25. On the other hand, the approach is clearly dependent on this degree.

9. Connection with RG flows

We expect similar features in higher dimensional scalar field theory with a UV regulator. Generically, a modified perturbative calculation involves some low-order coefficients with

Table 3. The estimators $a_k^{(2)}, b_k^{(2)}$ and $c_k^{(2)}$ for a λx^6 (above) and a λx^8 (below) perturbation. Unless specified, an error of 1 or less on the last printed digit is assumed.

k	$a_k^{(2)}$	$b_k^{(2)}$	$c_k^{(2)}$
		λx^6	
8	−1.79	−0.83	0.70
9	−1.69	−0.76	0.45
10	−1.57	−0.8	0.31
11	−1.46	−0.87	0.241
12	−1.38	−0.94	0.206(2)
13	−1.32	−0.99	0.187(2)
14	−1.30	−1.00	0.181
		λx^8	
8	4.0(3)	−6.2(3)	0.014
9	2.9	−5.1(2)	0.017
10	0.48	−2.65(4)	0.035
11	−0.44	−1.74(2)	0.055
12	−0.85	−1.33	0.076
13	−1.08	−1.12	0.095
14	−1.22	−0.979	0.11

Table 4. The estimators $\widehat{b}_k^{(3)}$ and $\widehat{c}_k^{(3)}$ for a λx^6 (above) and a λx^8 (below) perturbation. Unless specified, an error of 1 or less on the last printed digit is assumed.

k	$\widehat{b}_k^{(3)}$	$\widehat{c}_k^{(3)}$
	λx^6	
8	0.73	0.77
9	0.67	0.73
10	0.64	0.711
11	0.63	0.702
12	0.63	0.700
13	0.63	0.700
14	0.63	0.700
	λx^8	
8	0.45	0.619
9	0.45	0.624
10	0.46	0.629
11	0.46	0.633
12	0.46	0.637
13	0.47	0.640
14	0.47	0.644

values close to their usual ones, a few coefficients in the crossover region, and the rest of the coefficients taking values much smaller than in regular perturbation theory. These three regimes are reminiscent of the three regimes encountered when calculating renormalization group flows between two fixed points [11–14]. In addition, the approximate duality of equation (32) reminds us of the duality between fixed points of a simplified renormalization group equation [15] or the exchange between the perturbative and non-perturbative sectors of quasi-exactly solvable periodic potentials [16].

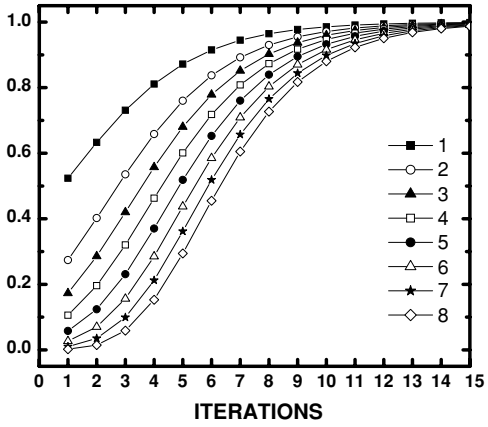

Figure 9. The first eight perturbative coefficients of the zero-momentum two-point function of the $D = 3$ hierarchical model, in units of their final values as a function of the number of iterations.

Intuitively, this suggests a connection between the crossover observed in the behaviour of the perturbative coefficients and the crossover behaviour of the RG flows. Our intuitive picture is as follows. When we construct numerically the RG flows starting near the Gaussian fixed point and let them evolve towards the high-temperature (HT) fixed point, it should be possible to describe the first iterations using the Gaussian scaling variables at low order. On the other hand, after a large number of iterations, the scaling variables of the HT fixed point are the relevant ones. If we use regular perturbation theory, we expect that it will be impossible to find a region where the two expansions are valid due to the zero radius of convergence of the weak coupling expansions [17]. On the other hand, if a field cut is introduced, the weak series have a non-zero radius of convergence and the direct calculations of critical amplitude, as in [13], might be possible. A generic feature that we then expect is that if we calculate the perturbative coefficients with a field cut, by block spinning, the first coefficients should stabilize quickly, while the large order in perturbation should stabilize after more iterations.

We have used an example where the block spin transformation can be performed easily and accurately, namely Dyson's hierarchical model [18]. The free parameter of this model has been tuned in order to mimic a three-dimensional model (see [19] for calculational details). The first eight coefficients of the zero-momentum two-point function as a function of the number of iterations of the block spin procedure are shown in figure 9 in units of their asymptotic values. One can see that as the order increases, the coefficients take more iterations to stabilize in agreement with the intuitive picture discussed above. This graph has been plotted for a particular field cut. If we reduce the value of the field cut, the curves move apart. For a sufficiently small field cutoff it is possible to find a correspondence between a given order in perturbation theory and the number of iterations for which the corresponding coefficient reaches a given fraction of its asymptotic value. We hope that a better understanding of this correspondence could lead to a quantitative explanation of the observations made in the previous chapters.

10. Conclusions

In summary, we have considered the simplest field theoretical models with a field cutoff, in zero and one dimension. We found in both cases that the crossover behaviour of the perturbative

coefficient can, for orders large enough, be described in a good approximation by rescaling and translating a universal (order-independent) function. Furthermore, this function can be expressed as a Gaussian integral. This statement is exact for the simple integral (in the sense of equation (14)). For the anharmonic oscillator, small non-Gaussian corrections persisting at large order cannot be completely ruled out. The coefficient of the quadratic term of the Gaussian was estimated to be 1.5, 1.3 and 1.2 for a λx^4, λx^6 and λx^8 perturbation respectively. The errors on these numerical values are difficult to estimate. Using the differences between successive values of the estimators as a guide, errors of order 0.1 are not unplausible. Simple possibilities such as a common coefficient close to 1.25 for all λx^{2N} perturbations or a coefficient decreasing with N are not excluded by our study. A more intensive calculation for larger order, larger $x_{\max}$ and smaller $\Delta x_{\max}$ could provide an answer to this question. A more interesting way to proceed might be to study the effect of the field cut on the dispersion relations of [20]. Finally, a similar study for Dyson's hierarchical model could provide a renormalization group explanation of the universality described in our paper.

Acknowledgments

This research was supported in part by the Department of Energy under contract no FG02-91ER40664 and also by the Obermann Center for Advanced Studies at the University of Iowa.

References

[1] Orland P and Xiao J 2005 *Phys. Rev.* B **72** 052503 (*Preprint* cond-mat/0503728)
[2] Altschul B 2005 *Preprint* quant-ph/0507252
[3] Li L and Meurice Y 2005 *J. Phys. A: Math. Gen.* **38** 8139 (*Preprint* hep-th/0506038)
[4] Li L and Meurice Y 2005 *Phys. Rev.* D **71** 054509 (*Preprint* hep-lat/0501023)
[5] Pernice S and Oleaga G 1998 *Phys. Rev.* D **57** 1144
[6] Meurice Y 2002 *Phys. Rev. Lett.* **88** 141601 (*Preprint* hep-th/0103134)
[7] Kessler B, Li L and Meurice Y 2004 *Phys. Rev.* D **69** 045014 (*Preprint* hep-th/0309022)
[8] Friedlander L 1985 *J. Math. Phys.* **26** 961
[9] Reed M and Simon B 1978 *Methods of Modern Mathematical Physics: IV Analysis of Operators* (San Diego, CA: Academic)
[10] Bender C M and Wu T T 1976 *Phys. Rev. Lett.* **37** 117
[11] Bagnuls C and Bervillier C 2002 *Phys. Rev.* E **65** 066132 (*Preprint* hep-th/0112209)
[12] Pelissetto A, Rossi P and Vicari E 1998 *Phys. Rev.* E **58** 7146
[13] Meurice Y and Niermann S 2002 *J. Stat. Phys.* **108** 213 (*Preprint* cond-mat/0105380)
[14] Tomboulis E T 2004 *Nucl. Phys. Proc. Suppl.* **129** 724 (*Preprint* hep-lat/0309006)
[15] Meurice Y and Niermann S 1999 *Phys. Rev.* E **60** 2612
[16] Dunne G V and Shifman M 2002 *Ann. Phys.* **299** 143 (*Preprint* hep-th/0204224)
[17] LeGuillou J C and Zinn-Justin J 1990 *Large-Order Behavior of Perturbation Theory* (Amsterdam: North-Holland)
[18] Dyson F 1969 *Commun. Math. Phys.* **12** 91
[19] Godina J, Meurice Y, Oktay M and Niermann S 1998 *Phys. Rev.* **57** 6326
[20] Bender C M and Wu T T 1973 *Phys. Rev.* D **7** 162O